Catalysis Today 141 (2009) 34–42

Contents lists available at ScienceDirect

Catalysis Today

journal homepage: www.elsevier.com/locate/cattod

Preparation of highly active catalysts for ultra-clean fuels☆

Naoto Koizumi, Takehisa Mochizuki, Muneyoshi Yamada *

Department of Applied Chemistry, Graduate School of Engineering, Tohoku University, Aoba 6-6-07, Aramaki, Aoba-ku, Sendai 980-8579, Japan

ARTICLE INFO

Article history:
Available online 9 May 2008

Keywords:
Fischer–Tropsch synthesis
Co/SiO_2 catalyst
Chelating agents

ABSTRACT

Novel preparation methods with chelating agents for Co/SiO_2 Fischer–Tropsch synthesis (FTS) catalysts were developed in the present study. The preparation with chelating agents such as nitrilotriacetic acid (NTA) or *trans*-1,2-diaminocyclohexane-*N*,*N*,*N*′,*N*′-tetra-acetic acid (CyDTA) greatly improved the FTS activity of Co/SiO_2 catalyst. The surface structures of the reduced and calcined catalysts were also investigated by means of various characterization techniques. Based on these results, it was suggested that the control of the interaction between Co^{2+}, chelating agents and SiO_2 surface was crucial to the preparation of Co/SiO_2 catalyst with higher FTS activity.

1. Introduction

Because of increasing demands for high-quality clean diesel fuels, many studies on both fundamental and technological aspects of Co-based Fischer–Tropsch synthesis (FTS) catalysts have been made in order to improve their activities and selectivities [1–7].

Co-based catalysts are usually prepared by an impregnation method followed by drying, calcination and H_2 reduction [1]. Co nitrate, a conventional Co precursor, is considered to decompose to Co_3O_4 species by drying and calcination [6–8]. During H_2 reduction, the Co_3O_4 species are reduced to CoO species and then successively reduced to metallic Co or Co–SiO_2 interaction species [9–12]. Iglesia et al. [2] have reported that the dispersion of metallic Co species correlates well with its FTS activity. Although it has been often reported that the dispersion of metallic Co species (i.e. the FTS activity) depends on Co precursors, pH of impregnating solution, and calcination temperatures, the detail mechanism of these dependencies is not known [13–15]. For example, it has been reported that CO conversion over Co/SiO_2 catalyst is improved by a factor of 1.4 when Co nitrate is co-impregnated with Co acetate, whereas the impregnation of Co nitrate and/or Co acetate alone results in lower conversions [13,14]. Since Co acetate is known to form highly dispersed Co oxide species that is hard to be reduced by H_2, the high activity induced by co-impregnation is interesting. However, the detail mechanism is still unclear. Kraum and Baerns [16] have reported that Co/TiO_2 catalysts prepared with Co acetate, Co acetylacetonate and/or Co oxalate show higher FTS activities than the catalyst prepared with Co nitrate. CO conversion over the catalysts prepared with these organic precursors is in a range from 23.6 to 32.0%, which is ca. 1.6–2.2 times higher than that over the catalyst prepared with Co nitrate. Although, the detail mechanism of these phenomena is still unclear, these works suggest that the use of organic Co compounds and organic Co complex strongly affects the dispersion of Co oxide species after drying and calcinations.

On the other hand, the authors have already found that hydrodesulfurization (HDS) activities of Co (or Ni) Mo (or W)/Al_2O_3 are highly improved when some chelating agents are added in impregnating solutions containing Co (or Ni) ions and Mo (or W) ions [17–22]. It was also found that the stability of the complexes strongly affects the HDS activity after presulfiding treatment. The role of chelating agents is considered to form stable complexes with Co^{2+} and to control the timing of sulfidation of Co.

Considering these previous studies, it is expected that some chelating agents affect the dispersion of Co species on the SiO_2 surface through formation of complexes with Co^{2+}. In order to improve the FTS activity of Co/SiO_2 catalyst, the FTS activity and selectivity of Co/SiO_2 catalysts prepared with some organic acids and chelating agents having various complex formation constants with Co^{2+} were investigated in the present study [23]. The surface structure of the prepared catalysts was also investigated to make clear their roles during the catalyst preparation [23,24].

2. Experimental

2.1. Preparation of catalysts

All the catalysts investigated here were prepared by pore-filling incipient wetness method. Two different types of impregnation methods, i.e. co-impregnation and stepwise impregnation meth-

☆ This forms part of the plenary lecture delivered in the symposium.

* Corresponding author.
E-mail address: yamada@erec.che.tohoku.ac.jp (M. Yamada).

0920-5861/$ – see front matter © 2008 Elsevier B.V. All rights reserved.
doi:10.1016/j.cattod.2008.03.020

Table 1
Organic acids and chelating agents used for the preparation of catalysts and their logarithmic complex formation constants with Co^{2+} ($\log K_{Co}$) [25–28]

Compound (notation)	$\log K_{Co}$
Organic acid	
Glycine (glycine)	0.6
Citric acid (citric)	5.0
L-Asparatic acid (asparatic)	5.9
Chelating agents	
Nitrilotriacetic acid (NTA)	10.4
Ethylenediamine-*N*,*N*,*N*′,*N*′-tetra-acetic acid (EDTA)	16.3
trans-1,2-Diaminocyclohexane-*N*,*N*,*N*′,*N*′-tetra-acetic acid (CyDTA)	18.9
Triethylenetetramine-*N*,*N*,*N*′,*N*″,*N*‴,*N*‴-hexa-acetic acid (TTHA)	28.8

ods, were utilized for the preparation of catalysts. In both cases, Sieved SiO_2 powder (JRC-SIO-5, BET surface area = 192 $m^2\,g^{-1}$, pore volume = 1.03 mL g^{-1}, (150–250) × 10^{-6} m powder) was used as a catalyst support and calcined at 823 K before use. Each method consists of the following procedures.

2.1.1. Co-impregnation method

Sieved SiO_2 powder was impregnated with an aqueous solution containing both $Co(NO_3)_2{\cdot}6H_2O$ (Wako Pure Chemicals, purity > 99.5%) and one of organic acids and/or chelating agents shown in Table 1. Unless otherwise stated, molar ratio of organic acids or chelating agents to Co^{2+} was unity for these aqueous solutions. The pH of the impregnating solutions was maintained at 9–10 (at room temperature) by using an aqueous NH_3 solution (Wako Pure Chemicals, 28 vol% NH_3) for all the catalysts with chelating agents because these chelating agents selectively form the complexes with Co^{2+} under this pH value. The impregnated sample was then dried at 393 K for 12 h and calcined at 723 K for 4 h in static air. Co loading of these catalysts is limited to a maximum of 5 mass% (as metallic Co) because it is difficult to prepare the homogeneous solutions of Co nitrate and organic acids or chelating agents having higher Co^{2+} concentrations. The catalysts thus prepared are denoted as L-Co(5)/SiO_2 (L = organic acids or chelating agents) in this paper.

2.1.2. Stepwise impregnation method

Sieved SiO_2 powder was firstly impregnated with the aqueous solution containing nitrilotriacetic acid (NTA) and/or *trans*-1,2-diaminocyclohexane-*N*,*N*,*N*′,*N*′-tetra-acetic acid (CyDTA) followed by drying at 393 K and 12 h. Dried material was subsequently impregnated with the aqueous $Co(NO_3)_2{\cdot}6H_2O$ solution with different Co^{2+} concentrations followed by drying (393 K and 12 h) and calcination (723 K and 4 h). The ratio of Co^{2+} to the chelating agents was varied in a range from 1 to 32 mol mol^{-1} by changing the loadings of Co or the chelating agents. In this paper, the catalysts thus prepared are denoted as Co(X)/L/SiO_2 (L = NTA or CyDTA, X = Co loading as metallic Co).

2.2. Activity measurements

FTS activities and selectivities of prepared catalysts were investigated using a fixed bed reactor. The reactor consisted of a stainless steel tube with an internal diameter of 7 mm in an electronically heated oven. Two sets of temperature controllers and thermocouples regulated the temperature in the catalyst bed within ±1 K. The gases, H_2 (purity > 99.995%) and 33% CO/62% H_2/5% Ar (purity > 99.99995%), were used without further purification in the reaction. The flow rate and the pressure of these gases were regulated with mass flow controllers (Brooks, 5850E) and a back-pressure regulator (TESCOM). Typically, 0.3 g of the calcined catalyst mixed with glass beads was charged into the reactor, and then reduced in a stream of H_2 at 773 K for 6 h. After H_2 reduction, the temperature was down to room temperature in H_2 stream. The feed gas was changed into CO/H_2/Ar at the pressure of 1.1 MPa with the flowing rate of 30 mL (STP) min^{-1} (W/F = 1.25 or 5.0 g-cat h $mol\text{-}CO^{-1}$). The catalyst was heated to 503 K at the heating rate of 2.5 K min^{-1} for the activity evaluation.

Gaseous products were periodically sampled with computer-controlled gas samplers and analyzed with two on line GCs after the reaction temperature reached 503 K. CO, CO_2 and CH_4 were quantified with the on line GC/TCD (Shimadzu, GC-8A), while C_1–C_7 hydrocarbons were quantified with the on line GC/FID (Shimadzu, GC-14B). Ar was used as an internal standard for the quantification with GC/TCD. Liquid products were collected with an ice trap during on stream and analyzed with off line GC/FID (Shimadzu, GC-17A) after the reaction. Temperature programmed GC analysis with a high-resolution capillary column (Supelco, Petrocol DH, 100 m × 0.25 mm) was employed for the separation of hydrocarbons in the liquid product. The chain growth probability (α) of hydrocarbons was calculated from the molar fraction of C_{10-20} hydrocarbon.

2.3. Characterization of catalysts

2.3.1. Characterization of the calcined catalysts

Bulk and subsurface structures of the calcined catalysts were investigated by X-ray diffraction (XRD) analysis and X-ray photoelectron spectroscopy (XPS).

XRD analysis was carried out on a MiniFlex diffractometer (RIGAKU). Cu Kα radiation was used as X-ray source generated from an X-ray tube operated at 30 kV and 15 mA. Diffraction intensities were recorded from 30° to 70° at the rate of 2.00° min^{-1} with the sampling width of 0.02°. The observed diffraction peaks were assigned by referring the Joint Committee on the Powder Diffraction Standards (JCPDS) card.

XPS spectra of the calcined catalysts were measured on an ESCA200 spectrometer (SIENTA). A monochromatized Mg Kα line was used as an excited source. The pass energy and the energy step were 150 and 0.05 eV, respectively, for all the measurements. Charge shift was corrected using C 1s binding energy (284.6 eV) as an internal standard. Background was subtracted from the spectrum using Shirley equation. The obtained spectrum was further deconvolved using Gauss function to quantify chemical species present in the subsurface region.

2.3.2. Characterization of the reduced catalysts

The calcined catalyst was reduced in a stream of H_2 at the same conditions as used for the activity measurements. After H_2-reduction, the catalyst was passivated in a stream of 1% O_2/He stream at room temperature, and then subjected to H_2 uptake measurements. H_2 uptakes of the reduced catalysts were measured by a volumetric method using AUTOSORB-1-C analyzer (Quantachrome INSTRUMENTS). H_2 adsorption was carried out at 373 K after *in situ* re-reduction at 573 K for 2 h in the adsorption cell.

2.3.3. Temperature programmed oxidation combined with mass spectroscopy

The decomposition and/or combustion processes of Co precursor during the calcination step were investigated by the temperature programmed oxidation combined with mass spectroscopy (TPO–MS). A conventional flow apparatus combined with an online mass spectrometer was used for this measurement. The dried catalyst (ca. 0.1 g) was charged in a quartz reactor (i.d. = 4 × 10^{-3} m, L = 250 × 10^{-3} m), and heated in 20% O_2/He stream from 300 to 800 K at a rate of 5 K min^{-1}. Products formed during the calcination were monitored by the online mass spectrometer.

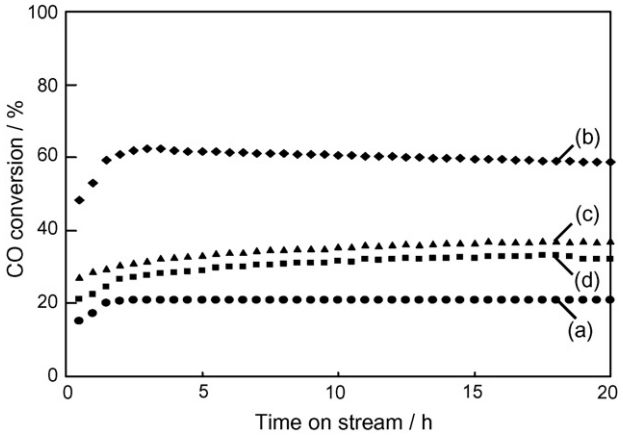

Fig. 1. Time-dependent behaviors of CO conversion over the reduced catalysts: (a) $Co(5)/SiO_2$, (b) NTA–$Co(5)/SiO_2$, (c) EDTA–$Co(5)/SiO_2$ and (d) CyDTA–$Co(5)/SiO_2$. *Reaction conditions*: 503 K, 1.1 MPa, and 5.0 g-cat h mol-CO^{-1}.

3. Results and discussion

3.1. FTS activities and selectivities of Co/SiO_2 catalysts prepared by the co-impregnation method with NTA, EDTA and CyDTA

The present study investigated at first the FTS activity and selectivity of reduced $Co(5)/SiO_2$ catalysts prepared with some chelating agents (NTA, EDTA and CyDTA) in order to make clear their effects on the FTS activity of Co/SiO_2 catalyst.

Fig. 1 shows CO conversions over the catalysts reduced in the H_2 stream at 773 K as a function of time on-stream. CO conversion over $Co(5)/SiO_2$ firstly increase with increasing time on stream and reach to a steady-state value (ca. 20%) within 3 h on stream. The turnover frequency over this catalyst calculated from its H_2 uptake (see Section 3.3) was 86×10^{-3} s^{-1}, which is comparable or higher than those reported in the previous studies [2,14,25–27]. The catalysts with chelating agents show similar time dependent behavior. CO conversion at 20 h on stream increases in the following order: $Co(5)/SiO_2$ < EDTA–$Co(5)/SiO_2$, CyDTA–$Co(5)/SiO_2$ < NTA–$Co(5)/SiO_2$. NTA is in particular effective among the chelating agents investigated here. The conversion over NTA–$Co(5)/SiO_2$ is ca. 3 times higher than that over $Co(5)/SiO_2$. Such the large activity-enhancement has never been reported in the previous studies with the catalysts prepared from the organic Co precursors. For example, Sun et al. [14] reported that CO conversion over Co/SiO_2 catalyst prepared from the mixed salt of Co nitrate and Co acetate (CO conversion: 42.5%) is ca. 1.4 times higher than that over the catalyst prepared from Co nitrate alone (29.8%). For the TiO_2-supported catalysts, Kraum and Baerns [16] reported that CO conversion over the catalyst prepared from Co oxalate (CO converiosn: 32.0%) was ca. 2.2 times higher than that

Table 2
Effect of some chelating agents on the product selectivity over reduced Co/SiO_2 catalyst

	Product selectivity[a] (mol%)			$\alpha^{a,b}$
	CO_2	CH_4[c]	C_{5+}	
$Co(5)/SiO_2$	ND	7.1	77.3	0.87
NTA–$Co(5)/SiO_2$	0.7	8.4	72.4	0.82
EDTA–$Co(5)/SiO_2$	ND	7.7	75.2	0.83
CyDTA–$Co(5)/SiO_2$	ND	10.8	67.9	0.79

[a] CO conversion: 20 ± 3%.
[b] Calculated from the molar fraction of C_{10}–C_{20} hydrocarbon (the uncertainty was estimated within ±0.01).
[c] The uncertainty was estimated within ±1%.

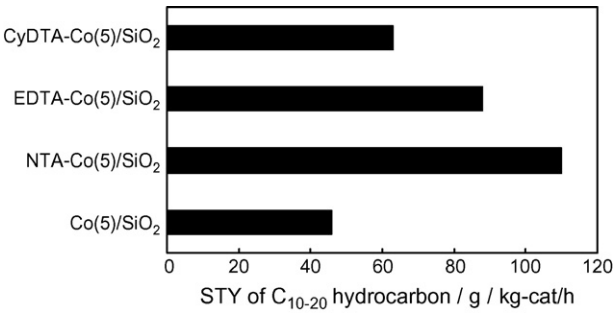

Fig. 2. Effects of some chelating agents on the space-time yield (STY) of C_{10}–C_{20} hydrocarbons obtained with reduced $Co(5)/SiO_2$ catalyst. *Reaction conditions*: 503 K, 1.1 MPa, and 5.0 g-cat h mol-CO^{-1}.

over the catalyst from Co nitrate (14.7%). It is also noted here that the preparation with EDTA results in the catalyst with relatively higher activity, which is in contrast to the previous results [15], where the use of Co-EDTA precursor instead of Co nitrate strongly depresses the conversion over Co/Al_2O_3 catalyst.

Table 2 summarizes the product selectivities together with chain growth probabilities of hydrocarbons over the reduced catalysts at ca. 20% CO conversion. Co/SiO_2 yields C_{5+} hydrocarbon with the selectivity of 77 C-mass%. The chain growth probability (α) of C_{10-20} hydrocarbon is 0.87. These values are comparable with those reported previously [14]. On the other hand, the selectivity for C_{5+} hydrocarbon over the catalysts with the chelating agents is lower than that over the catalyst without chelating agents. The α values for these catalysts are lower as well. Therefore, the preparation with these chelating agents suppresses the chain growth of the hydrocarbons. Fig. 2 compares the space-time yield (STY) of C_{10-20} hydrocarbon (equivalent to diesel fraction) over these catalysts. The STY of C_{10-20} hydrocarbon is higher for the catalysts with chelating agents. Especially, the preparation with NTA increased the STY of C_{10-20} hydrocarbons by a factor of ca. 3.

3.2. Effects of preparation conditions on the FTS activity of NTA–Co/SiO_2 catalyst

In order to obtain deeper understanding of the promoting effect of NTA, the FTS activity of NTA–$Co(5)/SiO_2$ catalysts prepared from

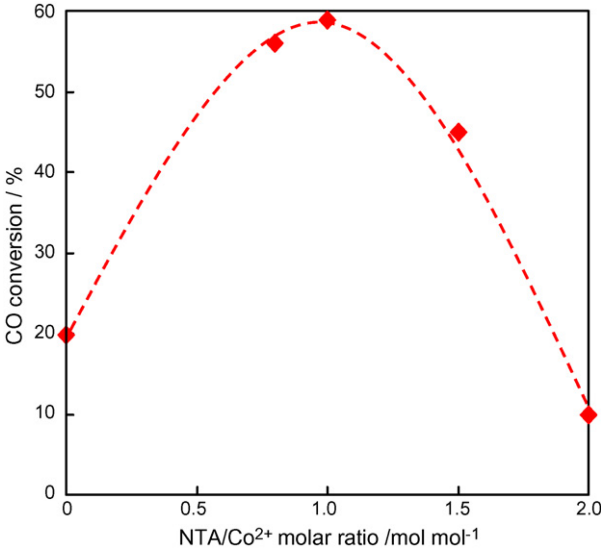

Fig. 3. CO conversion over reduced NTA–$Co(5)/SiO_2$ catalyst (at 20 h on stream) as a function of NTA/Co^{2+} molar ratio of the impregnating solution. *Reaction conditions*: 503 K, 1.1 MPa, and 5.0 g-cat h mol-CO^{-1}.

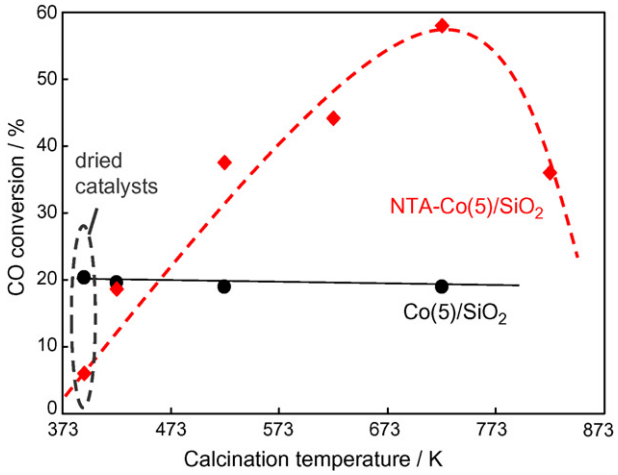

Fig. 4. Effect of the calcinations temperature on CO conversion over reduced NTA–Co(5)/SiO_2 and Co(5)/SiO_2 catalysts (at 20 h on stream). *Reaction conditions*: 503 K, 1.1 MPa, and 5.0 g-cat h mol-CO^{-1}.

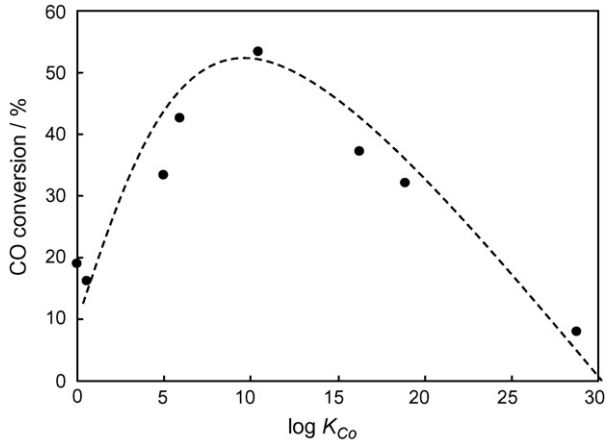

Fig. 5. Relationship between the FTS activity of the reduced catalysts (CO conversion at 20 h on stream) and the logarithmic complex formation constant of the organic acids and chelating agents used for the preparation of L-Co(5)/SiO_2 catalyst.

the impregnating solutions with different NTA/Co^{2+} molar ratios. Effect of the calcination temperature on the FTS activity was also investigated here.

Fig. 3 shows the steady-state CO conversion over NTA–Co(5)/SiO_2 catalyst as a function of NTA/Co^{2+} molar ratio of the impregnating solution. The concentration of NTA of the impregnating solution was varied here, while Co^{2+} concentration was kept constant. The conversion over this catalyst shows a broad maximum around NTA/Co^{2+} molar ratio of unity, suggesting that the formation of 1:1 complex in the impregnating solution is most effective for obtaining the higher FTS activity. It is worthy to note here that the impregnating solutions with NTA/Co^{2+} molar ratio above unity have large viscosities. This will suppress a uniform distribution of NTA–Co^{2+} complex in SiO_2 pores during the impregnation, which results in lower activities.

In Fig. 4, the conversion over Co(5)/SiO_2 and NTA–Co(5)/SiO_2 (NTA/Co^{2+} molar ratio = 1 mol mol^{-1}) catalysts is plotted as a function of the calcinations temperature [28]. This figure includes the conversions over the catalyst without calcination, where dried catalysts were directly reduced in H_2 stream at 773 K. Without calcination, Co(5)/SiO_2 catalyst shows ca 20% conversion. The conversion over this catalyst hardly depends on the calcination temperature. On the contrary, NTA–Co(5)/SiO_2 catalyst shows a quite low conversion (ca. 5%) without calcination. The conversion over this catalyst increases with increasing the calcination temperature up to 723 K. Higher conversions are obtained only when the catalyst is calcined above 523 K. In other words, NTA just works as an inhibitor when calcined at lower temperatures.

3.3. Effect of complex formation

The FTS activity of Co(5)/SiO_2 catalysts prepared with various organic acids or chelating agents was then investigated to make clear the effect of the complex formation on the FTS activity. The logarithmic complex formation constants of these organic acids and/or chelating agents with Co^{2+} lies in a range from 0.6 to 29 (Table 1) [29–32], which is suitable for investigating the effect of complex formation in the impregnating solution.

In Fig. 5, CO conversion over the prepared catalysts (at 20 h on stream) is plotted against the logarithmic complex formation constants of the organic acids and chelating agents used for the catalyst preparation. The conversion shows a maximum around the logarithmic complex formation constant of 10 (NTA). The preparation with the organic acids or chelating agents having much smaller and/or larger complex formation constants shows negligible and/or negative effects. This figure suggests that modification of the impregnating solution with the reagent having the appropriate complex formation constant with Co^{2+} is important for obtaining higher FTS activities of Co/SiO_2 catalyst. This result is important because L-Co/SiO_2 catalysts shown in Fig. 5 are prepared under the same conditions such as the pH of the impregnating solution and calcination conditions.

3.4. Dispersion of Co on the reduced catalysts

In order to investigate effects of the chelating agents and/or organic acids on the structure of metallic Co species, surface metallic Co sites were then titrated by H_2 uptake measurements. H_2 uptakes of the reduced catalysts are summarized in Table 3. H_2 uptakes of the catalysts with the chelating agents and/or organic acids (except for glycine and TTHA) are evidently larger than that of Co(5)/SiO_2 catalyst. Especially, H_2 uptake of NTA–Co(5)/SiO_2 catalyst is ca. 3 times larger than that of Co(5)/SiO_2 catalyst. The dispersion of Co, i.e. the number of surface metallic Co sites normalized to total amount of Co atoms in the reduced catalysts (Co_s/Co_{total}, where Co_s is the number of surface metallic Co sites and Co_{total} is the total amount of Co atoms in the reduced catalysts, Table 3) was calculated from H_2 uptakes of the reduced catalysts assuming that the stoichiometry for the hydrogen adsorption on the surface metallic Co sites is unity. The dispersion of Co is higher when the catalyst is prepared with the chelating agents and/or organic acids except for glycine and TTHA. Furthermore, the dispersion of Co increases in the same order as that for the CO conversion. It can be said that modification of the impregnating solution with some chelating agents and/or organic acids improves the dispersion of Co, leading to higher FTS activities.

Table 3
Effects of modification with the organic acids and/or chelating agents on H_2 uptake and the dispersion of Co over reduced Co/SiO_2 catalyst

	H_2 uptake (μmol-H_2 g^{-1})	Dispersion of Co (%)
Co/SiO_2	20.3	4.8
Glycine–Co/SiO_2	20.9	4.9
Citric–Co/SiO_2	39.4	9.3
Asparatic–Co/SiO_2	49.5	11.7
NTA–Co/SiO_2	65.0	15.3
EDTA–Co/SiO_2	37.9	8.9
CyDTA–Co/SiO_2	35.6	8.4
TTHA–Co/SiO_2	8.7	2.1

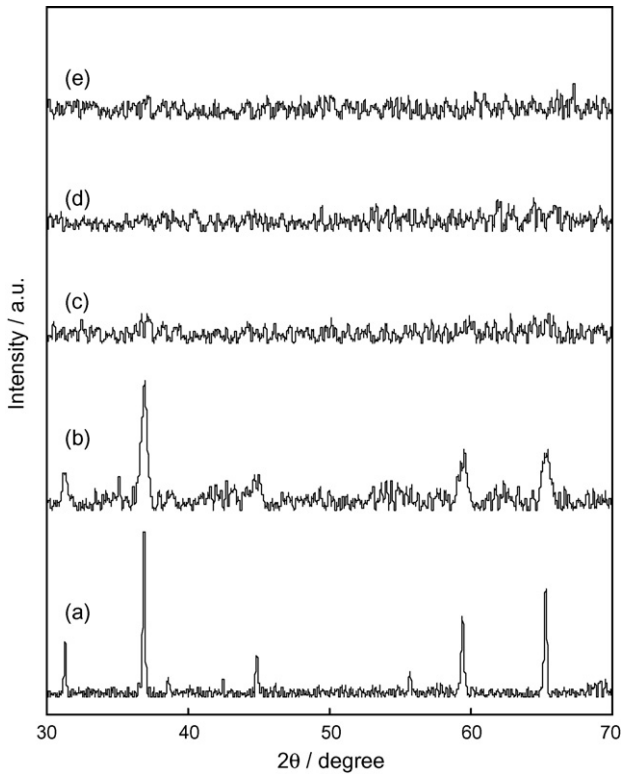

Fig. 6. XRD patterns of the calcined catalysts and polycrystalline Co_3O_4: (a) Co_3O_4, (b) Co(5)/SiO_2, (c) NTA–Co(5)/SiO_2, (d) EDTA–Co(5)/SiO_2, and (e) CyDTA–Co(5)/SiO_2.

3.5. Surface structure of the calcined catalysts

Then, the surface structures of the calcined catalysts were investigated in order to make clear why modification of the impregnating solution with some chelating agents improves the dispersion of Co. This was carried out to investigate bulk and subsurface structures of the calcined catalysts with or without chelating agents (NTA, EDTA and CyDTA).

3.5.1. Bulk structure

Fig. 6 shows XRD patterns of the calcined catalysts and polycrystalline Co oxide (Co_3O_4). Broad diffraction peaks are observed in the XRD pattern of the calcined Co(5)/SiO_2 in the range from 30° to 70°. 2θ values of these peaks are consistent well with those observed for Co_3O_4. On the other hand, no diffraction peaks are observed when the catalyst was prepared with chelating agents.

3.5.2. Subsurface structure

XPS measurements were then carried out in order to obtain more quantitative information about the surface structure of the calcined catalysts. Figs. 7 and 8 show XPS spectra of the calcined catalysts in Co 2p region and binding energies of Co $2p_{3/2}$ peaks for the calcined catalysts, respectively. In Fig. 7, the spectra of the polycrystalline Co oxides (Co_3O_4, CoO and α-Co_2SiO_4 [28]) are shown as references. In the spectra of CoO and Co_3O_4, Co $2p_{3/2}$ peaks are observed at 778.5 eV (CoO) and 778.6 eV (Co_3O_4), respectively, with satellite peaks at ca. 6 eV (CoO) and/or 9 eV (Co_3O_4) higher energy sides from their Co $2p_{3/2}$ peaks. Furthermore, the relative intensity of the satellite peak is stronger for CoO. These differences in the satellite peak are interpreted in terms of the difference in the distribution of Co ions (Co^{2+} and Co^{3+}) in tetrahedral and octahedral coordination sites in the subsurface region of Co_3O_4 and CoO [33]. Compared with these Co oxides, the

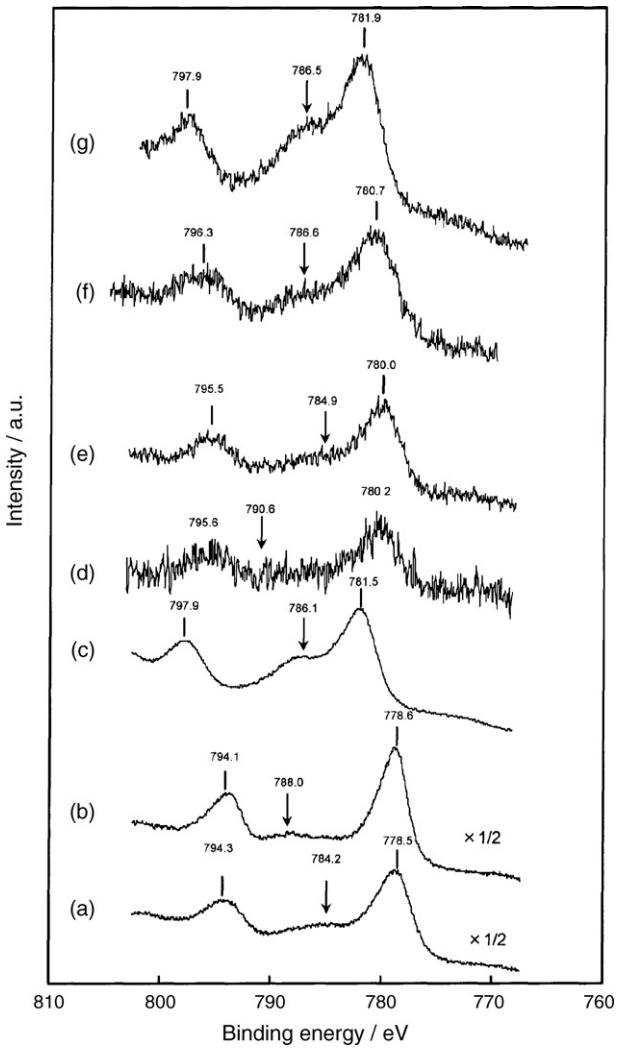

Fig. 7. XPS spectra in Co 2p region of the calcined catalysts and polycrystalline Co oxides: (a) CoO, (b) Co_3O_4, (c) α-Co_2SiO_4, (d) Co/SiO_2, (e) NTA–Co(f)/SiO_2, (f) EDTA–Co(5)/SiO_2, and (g) CyDTA–Co(5)/SiO_2 (arrows indicate the position of the satellite peak).

binding energy of Co $2p_{3/2}$ peak is evidently higher for α-Co_2SiO_4 (781.5 eV). Besides, the satellite peak in this spectrum (786.1 eV) is stronger than that in the spectrum of CoO. In comparison with these reference spectra, the structure of Co species on the calcined catalysts was further examined as follows.

3.5.2.1. Calcined Co(5)/SiO_2 catalyst. Co $2p_{3/2}$ peak appears at a higher energy than those for the polycrystalline Co oxides. Because XRD pattern of this catalyst is comparable with that of Co_3O_4, the higher binding energy of Co $2p_{3/2}$ peak could be attributed to the formation of some kind of interaction between SiO_2 support and Co_3O_4-like species [9]. The formation of Co_3O_4-like species is also consistent with weaker satellite peak observed at ca. 10 eV higher energy side from Co $2p_{3/2}$ peak like as Co_3O_4.

3.5.2.2. Calcined Co(5)/SiO_2 modified with chelating agents. For the calcined NTA–Co/SiO_2 catalyst, the binding energy of Co $2p_{3/2}$ peak is comparable with that for calcined Co/SiO_2 catalyst. However, relatively stronger satellite peak is observed ca. 5 eV higher energy side from Co $2p_{3/2}$ peak, which is characteristic of CoO rather than Co_3O_4. Considering the fact that XRD pattern of this catalyst shows no diffraction peaks, we can only say at present that Co oxide

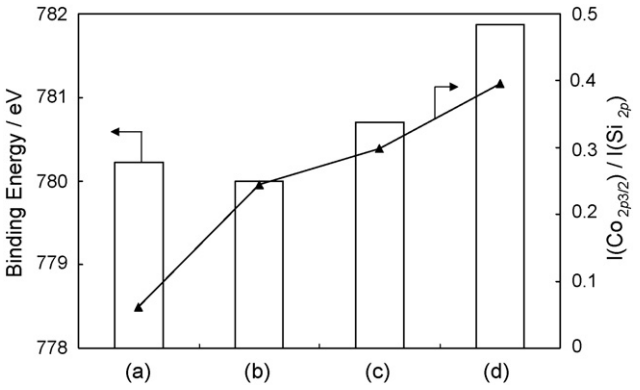

Fig. 8. Binding energy and intensity of Co $2p_{3/2}$ peak (normalized to Si 2p peak) in XPS spectra of the calcined catalyst: (a) Co(5)/SiO_2, (b) NTA–Co(5)/SiO_2, (c) EDTA–Co(5)/SiO_2, and (d) CyDTA–Co(5)/SiO_2.

species with unknown stoichiometry (denoted as CoOx species in this paper) is predominant in the subsurface region of calcined NTA–Co(5)/SiO_2 catalyst. On the contrary, the binding energy of Co $2p_{3/2}$ peak for the calcined CyDTA–Co(5)/SiO_2 catalyst (781.9 eV) is evidently higher than those for other catalysts. Furthermore, the satellite peak is clearly observed at 786.5 eV in this spectrum. These spectral features are characteristic of α-Co_2SiO_4 as described above. Therefore, there will mainly exists α-Co_2SiO_4-like species over this catalyst. In the case of the calcined EDTA–Co(5)/SiO_2 catalyst, the binding energy of Co $2p_{3/2}$ peak is in between those for calcined CyDTA–Co(5)/SiO_2 and NTA–Co(5)/SiO_2 catalysts. Furthermore, a full width at half maximum of Co $2p_{3/2}$ peak for the calcined EDTA–Co(5)/SiO_2 catalyst is greater than those for the other two catalysts. These results suggest that both α-Co_2SiO_4-like species and CoOx species are formed over the catalyst with EDTA.

Fig. 8 also summarizes the ratio of integrated intensities of Co $2p_{3/2}$ and Si 2p peaks (I(Co $2p_{3/2}$)/I(Si 2p)). It is worthy to note that I(Co $2p_{3/2}$)/I(Si 2p) is higher for the catalysts with chelating agents. Thus, Co species over the catalysts with chelating agents has smaller cluster sizes, which makes them difficult to detect by XRD analysis. Both XRD and XPS measurements show that the surface structure of the calcined catalyst is affected by the use of chelating agents. The use of different chelating agents results in Co species having different structures after the calcination, where dispersed CoOx species is mainly formed when modified with NTA.

3.6. Role of chelating agents

In the previous studies, several authors proposed the factors affecting the surface structure of the calcined catalyst. Based on TPR measurements, van Steen et al. [10] proposed that the ligand exchange reaction between Co aqua-complex and SiO^- groups during the impregnating step is responsible for the formation of the precursor of Co silicate. The formation of silicate-like species after the calcination strongly depends on the pH and/or the polarity of the impregnating solution according to their proposal, because the number of SiO^- groups changes depending on them. On the contrary, Girardon et al. [34] recently reported that the structure of Co species after the calcination depends on whether the decomposition of Co precursor is endothermic or exothermic during the calcination step, where Co_2SiO_4 is mainly formed after the calcination when the catalyst prepared from Co acetate instead of Co nitrate because of the exothermic decomposition by the combustion of the acetate skeleton. However, these previous studies cannot tell us why dispersed CoOx species is formed after the calcination when the impregnating solution is modified with NTA.

When we consider the role of the chelating agents, it should be noted that these chelating agents form stable complexes with Co^{2+} in the impregnating solution. Thermodynamic calculations in our previous study suggested that these complexes could survive during the drying step [22]. On the other hand, XPS analysis in the present study showed the absence of carbonaceous compounds originated from the chelating agents after the calcination (not shown here), suggesting the importance of phenomena during the drying and calcination steps. In order to examine this point further, TPO–MS measurements during the calcinations of dried Co(5)/SiO_2 and NTA–Co(5)/SiO_2 catalysts were also carried out here (Fig. 9). NOx (NO and NO_2) are evolved below 500 K during the calcinations of dried Co/SiO_2 catalyst, which is originated from the decomposition of nitrate species. On the contrary, strong COx (CO and CO_2) and NOx formations are observed as well around 600 K in the TPO–MS profile of dried NTA–Co/SiO_2 catalyst. Because CO_2 and NO_2 formations were mainly observed around 500 K when only NTA was impregnated onto SiO_2 support followed by drying (not shown here), it can be said that COx and NOx formations at higher temperature during the calcinations of dried NTA–Co(5)/SiO_2 catalyst are caused by the decomposition and/or combustion of NTA–Co^{2+} complex. These results support the hypothesis that the complex formation between Co^{2+} and NTA mainly affects the phenomena occurring during the drying and calcination steps, which results in the formation of dispersed CoOx species after the calcinations at higher temperature. It is probable that the complex between Co^{2+} and NTA formed in the impregnating solution prevents the sintering of Co species during the thermal treatment in the preparation steps, drying and calcination steps, because such the complex has a bulky structure. This capsulate effect of NTA will contribute to the formation of Co oxide species with more dispersed state after the calcination.

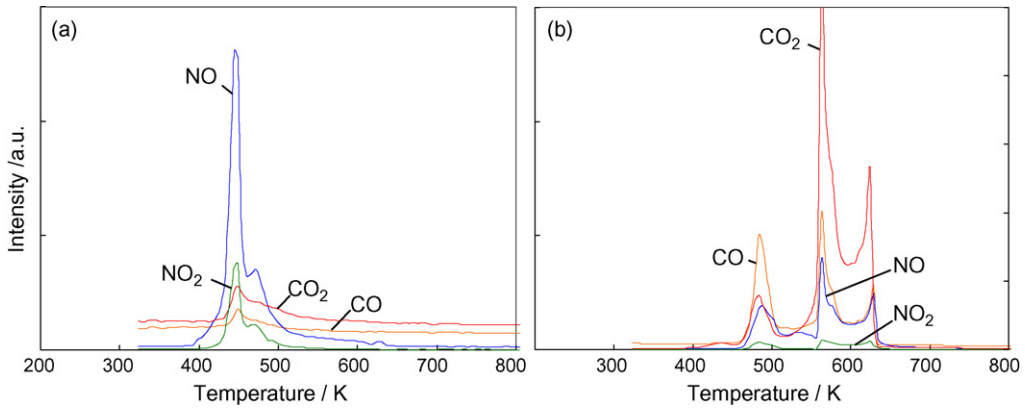

Fig. 9. TPO–MS profiles during the calcinations of dried Co(5)/SiO_2 (a) and NTA–Co(5)/SiO_2 (b) catalysts in 20% O_2/He stream (heating rate: 5 K min^{-1}).

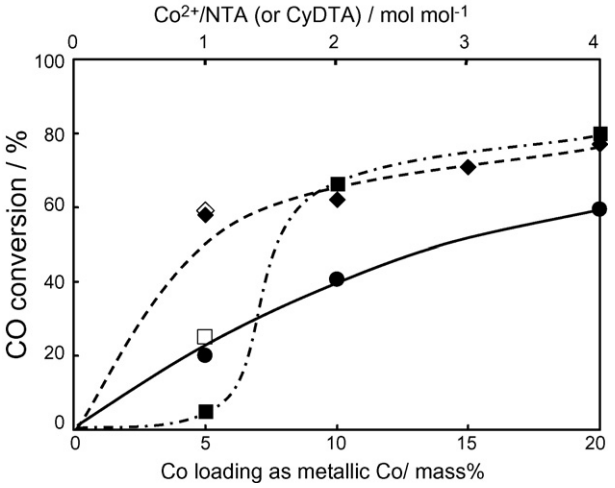

Fig. 10. Effect of Co loading on CO conversions over Co(X)/SiO_2 (●), Co(X)/NTA/SiO_2 (◆), and Co(X)/CyDTA/SiO_2 (■) catalysts. The conversions over NTA–Co(5)/SiO_2 (◇) and CyDTA–Co(5)/SiO_2 (□) catalysts are also plotted in this figure. NTA and CyDTA loadings were fixed at 16 and 31 mass%, respectively, for the catalysts prepared by the stepwise impregnation method. *Reaction conditions*: 503 K, 1.1 MPa, and 5.0 g-cat h mol^{-1}.

3.7. Preparation of Co/SiO_2 catalysts by the stepwise impregnation method with some chelating agents and their FTS activity

In order to investigate the role of these chelating agents from different point of view, the catalysts were further prepared by the stepwise impregnation of aqueous solutions containing Co nitrate or the chelating agent (NTA or CyDTA). The concentrations of Co^{2+} and the chelating agent (and thus the molar ratio of Co^{2+} to the chelating agent) were varied in a wide range here.

3.7.1. Effect of Co loading

Co loading of L-Co/SiO_2 catalyst is limited to a maximum of 5 mass% because it is difficult to prepare the homogeneous solutions of Co nitrate and the chelating agent having higher Co^{2+} concentrations. On the contrary, Co loading of the catalysts can be increased when the catalysts are prepared by the stepwise impregnation method with the chelating agent. Thus, effects of NTA and CyDTA on the FTS activity of the catalyst having higher Co loadings were further investigated at 503 K and 1.1 MPa with W/F = 5 g h mol^{-1}. Co loading was varied from 5 to 20 mass% as metallic Co, whereas the loading of the chelating agents was kept constant. In Fig. 10, CO conversions (at 20 h on stream) over Co(X)/SiO_2 and Co(X)/L/SiO_2 (L = NTA or CyDTA) catalysts are plotted as a function of their Co loading. This figure also includes the conversions over NTA–Co(5)/SiO_2 and CyDTA–Co(5)/SiO_2 catalysts as references. CO conversion over Co(X)/SiO_2 catalyst increases with increasing Co loading, and reaches to 60% at Co loading of 20 mass% as metallic Co. The conversion over Co(X)/NTA/SiO_2 catalyst is always higher than that over Co(X)/SiO_2 catalyst, and eventually reaches to ca. 80%. It is also noted that the conversions over Co(5)/NTA/SiO_2 and NTA–Co(5)/SiO_2 catalysts are comparable with each other (60%), showing that promoting effects of NTA are observed even though the catalysts are prepared by the stepwise impregnation method. On the contrary, the conversion is quite low over Co(5)/CyDTA/SiO_2 catalyst. This catalyst shows the lower conversion than CyDTA–Co(5)/SiO_2 catalyst. An abrupt increase in the conversion is observed over Co(X)/CyDTA/SiO_2 catalyst when Co loading increases from 5 to 10 mass%. The conversion further increases with Co loading, and reaches a similar level to Co(20)/NTA/SiO_2 catalyst. Both NTA and CyDTA show the promoting effects on the FTS activity of Co/SiO_2 catalyst having higher Co loadings (10–20 mass%). The stepwise impregnation method has important advantages that Co loading of the catalysts with NTA and/or CyDTA can be increased at least up to 20 mass%, and the promoting effects of these chelating agents are clearly observed for the catalyst having higher Co loadings.

3.7.2. STY of hydrocarbons

Table 4 summarizes the chain growth probabilities of hydrocarbons and STY of C_{10-20} hydrocarbon over Co(20)/NTA/SiO_2 and Co(20)/CyDTA/SiO_2 catalysts (Co^{2+}/NTA or CyDTA = 4 mol mol^{-1}) in comparison with those over Co(20)/SiO_2 catalyst. FTS reactions were carried out at W/F = 1.25 g h mol^{-1} because the conversions over Co(20)/NTA/SiO_2 and Co(20)/CyDTA/SiO_2 catalysts reach to 80% at W/F = 5 g h mol^{-1} (Fig. 10). The chain growth probability of C_{10-20} hydrocarbon (α) over Co(20)/SiO_2 catalyst is 0.85, whereas the α values over Co(20)/NTA/SiO_2 and Co(20)/CyDTA/SiO_2 catalysts are slightly lower. On the contrary, 608 and 1500 g kg-cat^{-1} h^{-1} of C_{5+} hydrocarbon are obtained with Co(20)/NTA/SiO_2 and Co(20)/CyDTA/SiO_2 catalysts, which is much greater than that with Co(20)/SiO_2 catalyst (360 g kg-cat^{-1} h^{-1}). Furthermore, the STY of C_{10-20} hydrocarbon (equivalent to the diesel fraction) reaches 815 g kg-cat^{-1} h^{-1} over Co(20)/CyDTA/SiO_2 catalyst. The STY of C_{5+} and C_{10-20} hydrocarbons obtained with this catalyst is ca. 4.3 and 7.4 times greater than those obtained with NTA–Co(5)/SiO_2 catalyst. These differences in the STY of hydrocarbons (Co(20)/CyDTA/SiO_2 vs. NTA–Co(5)/SiO_2) are evidently greater than those observed for the catalyst without chelating agents (Co(20)/SiO_2 vs. Co(5)/SiO_2).In open literatures, the champion data for the STY of C_{5+} and C_{10-20} hydrocarbons has been reported to be 710 and 350 g kg-cat^{-1} h^{-1}, respectively, over SBA-15 supported Co catalyst (Co loading: 20 mass% as metallic Co) at 503 K and 2.0 MPa with W/F of 2.4 g h mol^{-1} [35]. Co(20)/CyDTA/SiO_2 catalyst yields C_{5+} and C_{10-20} hydrocarbons more than two times greater than Co/SBA-15 catalyst even under lower reaction pressure.

3.7.3. Effect of NTA and CyDTA loadings

As shown in Fig. 3, it was suggested that the formation of 1:1 complex in the impregnating solution is responsible for the higher FTS activity of NTA–Co(5)/SiO_2 catalyst. In the present study, it was also found that the promoting effects of NTA and CyDTA are observed even though the catalysts were prepared by the stepwise

Table 4
Effects of NTA and CyDTA on the FTS selectivity and hydrocarbon productivity over the reduced Co catalysts prepared by the stepwise impregnation method[a]

	W/F (g-cat h mol-CO^{-1})	CO conversion (%)	α[b]	STY of C_{5+} (g kg-cat^{-1} h^{-1})	STY of C_{10}–C_{20} (g kg-cat^{-1} h^{-1})
Co(5)/SiO_2	5	19	0.87	145	46
Co(20)/SiO_2	1.25	19	0.85	360	209
NTA–Co(5)/SiO_2	5	53	0.82	348	110
Co(20)/NTA/SiO_2[c]	1.25	30	0.83	608	270
Co(20)/CyDTA/SiO_2[c]	1.25	60	0.81	1500	815

[a] *Reaction conditions*: 503 K and 1.1 MPa.
[b] Calculated from the molar fraction of C_{10}–C_{20} hydrocarbon (the uncertainty was estimated within ±0.01).
[c] Co^{2+}/NTA or CyDTA = 4 mol mol^{-1}.

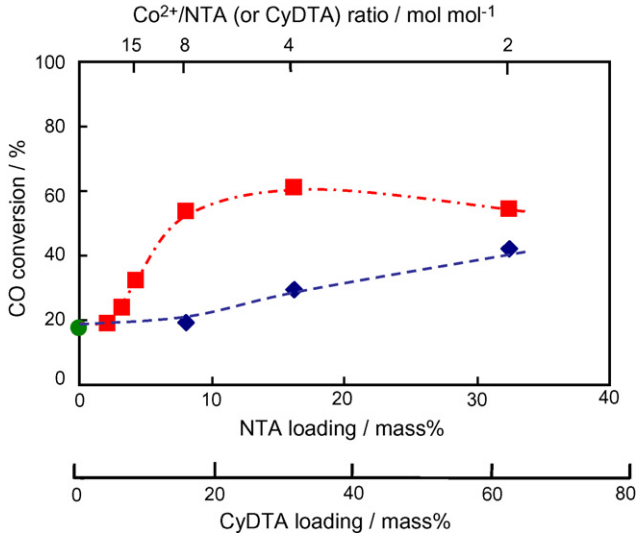

Fig. 11. Effect of NTA and CyDTA loadings on CO conversions over Co(20)/NTA/SiO_2 (◆) and Co(20)/CyDTA/SiO_2 (■) catalysts. *Reaction conditions*: 503 K, 1.1 MPa, and 1.25 g-cat h mol^{-1}.

impregnation method as mentioned above. In order to investigate the role of these chelating agents in view of the complex formation, the FTS activities of Co(20)/NTA/SiO_2 and Co(20)/CyDTA/SiO_2 catalysts having various Co^{2+}/L (L = NTA or CyDTA) molar ratios were further investigated. In these experiments, the loadings of NTA and CyDTA were varied, while Co loading was kept constant (20 mass% as metallic Co). It should be noted that the catalysts having the Co^{2+}/L molar ratio below 2 mol mol^{-1} could not be prepared because of difficulties in the preparation of homogenous solutions containing these chelating agents at higher concentrations. Their FTS activities were evaluated at W/F = 1.25 g h mol^{-1}. Obtained results are summarized in Fig. 11. Over Co(20)/NTA/SiO_2 catalyst, CO conversion gradually increases with increasing NTA loading (Co^{2+}/NTA molar ratio from 15 to 2 mol mol^{-1}). On the contrary, CO conversion over Co(20)/CyDTA/SiO_2 catalyst steeply increases at CyDTA loading of 8 mass% (Co^{2+}/CyDTA = 15 mol mol^{-1}). The conversion over this catalyst shows a broad maximum in a wide range of CyDTA loading (Co^{2+}/CyDTA molar ratio from 8 to 2 mol mol^{-1}). These two catalysts show different dependencies upon the Co^{2+}/L molar ratio, and Co(20)/CyDTA/SiO_2 catalyst always shows higher conversions irrespective of this ratio. It is noted that this result is in contrast with the results for the co-impregnated catalysts, where the higher conversion was obtained by the catalyst with NTA rather than CyDTA when the catalyst is prepared from the aqueous solution containing Co nitrate and these chelating agents.

The increasing conversion over Co(20)/NTA/SiO_2 catalyst with decreasing the Co^{2+}/NTA molar ratio is consistent with the dependency observed for NTA–Co(5)/SiO_2 catalyst upon the Co^{2+}/NTA molar ratio. On the contrary, the conversion over Co(20)/CyDTA/SiO_2 catalyst shows a broad maximum in the wide range of the Co^{2+}/CyDTA molar ratio (8–2 mol mol^{-1}). Much smaller CyDTA is enough for obtaining a higher activity over this catalyst compared with the co-impregnated catalyst. Such the dependency upon the Co^{2+}/CyDTA molar ratio cannot be explained simply in terms of the stoichiometric 1:1 complex formation during the preparation step in the catalyst pores. It is suggested that the formation of a small amount of CyDTA–Co^{2+} complex affect the dispersion of Co species formed after the calcination, although detailed mechanism is still unclear yet.

4. Conclusion

The present study investigated the FTS activity and surface structure of reduced Co/SiO_2 catalysts prepared with some organic acids and/or chelating agents having various complex formation constants with Co^{2+}.

It was found that the preparation of Co/SiO_2 catalyst from the impregnating solution containing both Co nitrate and some organic acids or chelating agents improved its FTS activity. The complex formation constant of the organic acids and/or chelating agents was crucial to the FTS activity. Characterization studies on the reduced and calcined catalysts suggested that the preparation with the chelating agents increases the number of surface metallic Co sites through modification of the structure of Co species after the calcination, leading to the higher FTS activity. From these results, it was considered that the presence of the complex having moderate stability (i.e. NTA–Co^{2+} complex) on the dried catalyst is important for obtaining the higher FTS activity, although the presence of the complex is not verified by spectroscopic techniques.

Furthermore, chelating agent-modified catalysts having higher Co loadings (at least up to 20 mass%) could be prepared by the stepwise impregnation method. The promoting effects of NTA and CyDTA were clearly observed for these catalysts. The catalyst prepared by the stepwise impregnation method with CyDTA yielded 1500 and 815 g kg-cat^{-1} h^{-1} of C_{5+} and C_{10-20} hydrocarbons at 503 K and 1.1 MPa, respectively, which were much greater than those reported in the previous studies. It was found that much smaller CyDTA is enough for obtaining a higher activity compared with the co-impregnated catalyst (Co^{2+}/CyDTA molar ratio = 8–2 mol mol^{-1}), suggesting that the formation of a small amount of CyDTA–Co^{2+} complex affect the dispersion of Co species formed after the calcination. However, detailed mechanism is still unclear yet.

In summary, the present study clearly shows that there still exists a room to improve the FTS activity of Co/SiO_2 catalyst, although great efforts have been made so far to improve its activity. Detailed studies on the promoting mechanism of these chelating agents will contribute to further activity improvement in the FTS activity of Co catalysts.

Acknowledgement

This work was partly supported by the Ministry of Education, Culture, Sports, Science and Technology, a Grant-in-Aid for the 21st Century COE project, Giant Molecules and Complex Systems. This research was also supported by the Japan Society for the Promotion of Science (JSPS), Grant-in-Aid for Scientific Research (S), 17106011, 2005.

References

[1] R.C. Reuel, C.H. Bartholomew, J. Catal. 85 (1984) 78.
[2] E. Iglesia, S.C. Reyes, R.J. Madon, S.L. Soled, Adv. Catal. 39 (1993) 221.
[3] M.E. Dry, Appl. Catal. A: Gen. 138 (1996) 319.
[4] M.E. Dry, Catal. Today 71 (2002) 227.
[5] J. Ming, N. Koizumi, T. Ozaki, M. Yamada, Appl. Catal. A: Gen. 209 (2001) 59.
[6] G. Bian, N. Fujishita, T. Mochizuki, W. Ning, M. Yamada, Appl. Catal. A: Gen. 252 (2003) 251.
[7] G. Bian, T. Mochizuki, N. Fujishita, H. Nomoto, M. Yamada, Energy Fuels 17 (2003) 799.
[8] B. Ernst, A. Bensaddik, L. Hilaire, P. Chaumette, A. Kiennemann, Catal. Today 39 (1998) 329.
[9] H. Ming, B.G. Baker, Appl. Catal. A: Gen. 123 (1995) 23.
[10] E. van Steen, G.S. Sewell, R.A. Makhothe, C. Micklethwaite, H. Manstein, M. de Lange, C.T. O'Connor, J. Catal. 162 (1996) 220.
[11] K.E. Coulter, A.G. Sault, J. Catal. 154 (1992) 56.
[12] A.Y. Khodakov, J. Lynch, D. Bazin, B. Rebours, N. Zanier, B. Moisson, P. Chaumette, J. Catal. 168 (1997) 16.

[13] T. Matsuzaki, K. Takeuchi, T. Hanaoka, H. Arakawa, Y. Sugi, Appl. Catal. A: Gen. 105 (1993) 159.
[14] S. Sun, N. Tsubaki, K. Fujimoto, Appl. Catal. A: Gen. 202 (2000) 121.
[15] J. van de Loosderecht, M. van der Haar, A.M. van der Kraan, A.J. van Dillen, J.W. Geus, Appl. Catal. A: Gen. 150 (1997) 365.
[16] M. Kraum, M. Baerns, Appl. Catal. A: Gen. 186 (1999) 189.
[17] T. Shimizu, S. Kasahara, T. Kiyohara, K. Kawahara, M. Yamada, J. Jpn. Petrol. Inst. 38 (6) (1995) 384.
[18] K. Hiroshima, T. Kiyohara, N. Koizumi, T. Shimizu, M. Yamada, J. Jpn. Petrol. Inst. 40 (1997) 35.
[19] K. Hiroshima, T. Mochizuki, T. Honma, T. Shimizu, M. Yamada, Appl. Surf. Sci. 121/122 (1997) 433.
[20] T. Shimizu, K. Hiroshima, T. Honma, T. Mochizuki, M. Yamada, Catal. Today 45 (1998) 271.
[21] Y. Ohta, T. Shimizu, T. Honma, M. Yamada, Stud. Surf. Sci. Catal. 127 (1999) 161.
[22] H. Itou, N. Koizumi, N. Sakamoto, T. Honma, M. Shingu, M. Yamada, J. Jpn. Petrol. Inst. 47 (4) (2004) 249.
[23] T. Mochizuki, T. Hara, N. Koizumi, M. Yamada, Catal. Lett. 113 (2007) 165.
[24] T. Mochizuki, T. Hara, N. Koizumi, M. Yamada, Appl. Catal. A: Gen. 317 (2007) 97.
[25] A. Feller, M. Claeys, E. van Steen, J. Catal. 185 (1999) 120.
[26] S. Stors[]ter, Ø. Borg, B.A. Holmen, J. Catal. 231 (2005) 405.
[27] G.L. Benzemer, J.H. Bitter, H.P.C.E. Kuipers, H. Oosterbeek, J.E. Holewijn, X. Xu, F. Kapteijn, A.J. von Dillen, K.P. de Jong, J. Am. Chem. Soc. 128 (2006) 3956.
[28] T. Mochizuki, N. Koizumi, Y. Hamabe, T. Hara, H. Takizawa, M. Yamada, J. Jpn. Petrol. Inst. 50 (5) (2007) 262.
[29] G. Scwarzenbach, R. Gut, G. Anderegg, Helv. Chim. Acta 37 (1954) 937.
[30] L.G. Sillen, A.E. Martell, Stability Constants of Metal Ligand Complexes, The Chemical Society, London, 1964.
[31] L.G. Sillen, A.E. Martell, Stability Constants Supplement 1, The Chemical Society, London, 1968.
[32] A.E. Martell, R.M. Smith, Critical Stability Constants, vol. 5, Plenum Press, New York, 1982.
[33] T.J. Chuang, C.R. Brundle, D.W. Rice, Surf. Sci. 59 (1976) 413.
[34] J.S. Girardon, A.S. Lermontov, L. Gengembre, P.A. Chernavskii, A.G. Constant, A.Y. Khodakov, J. Catal. 230 (1992) 339.
[35] Y. Ohtsuka, T. Arai, S. Takasaki, N. Tsubouchi, Energy Fuels 17 (2003) 804.